Solubility-Controlled Structural Ordering of Narrow Bandgap Conjugated Polymers

*Yeong Don Park, Jin Kuen Park, Jung Hwa Seo, Jonathan D. Yuen, Wi Hyoung Lee, Kilwon Cho, and Guillermo C. Bazan**

Organic semiconductors based on π-delocalized conjugated polymers are under consideration for a variety of emerging optoelectronic technologies.[1–10] These materials open the possibility of solution processing and thereby manufacturing options not easily achieved with their inorganic semiconductor counterparts. However, because interchain forces arise predominantly from weak van der Waals interactions, one finds that not only is the molecular structure of the polymer important for determining structural, optical and electronic properties, but also the processing history. The result is that a wide performance range can be achieved for a given polymer sample depending on the choice of solvent, deposition method and thermal management history. This complexity invites research into understanding how to control supramolecular structures[11] and how charge transport can be modified by the general organization of conjugated polymers in the bulk and adjacent to device interfaces.[12]

Structural defects within the semiconductor layer of field effect transistors (FETs) due to poorly organized arrangements can be a major challenge for obtaining high-performance devices. Charge-carrier transport is limited via hopping between molecules in disordered regions with weak intermolecular electronic coupling.[13,14] Morphology control is even more demanding in bulk heterojunction solar cells, where bicontinuous networks of donor and acceptor semiconductor phases need to be appropriately arranged within an ~100 nm thick active layer to optimize the power conversion efficiency of the devices.[15,16] A number of processing options exist, including choice of solvent,[17–20] post-treatments such as thermal[21,22] or solvent annealing,[23–25] and film forming method.[26] However, a universal correlation between molecular structure, processing, film morphology, and device performance has not been attained.

In this contribution we disclose how to modify the morphological order of poly[(4,4-didodecyldithieno[3,2-*b*:2',3'-*d*]silole)-2,6-diyl-*alt*-(2,1,3-benzothiadiazole)-4,7-diyl] (**P1** in **Figure 1**a) by aging solutions in a solvent of marginal quality. The assembly of chains in solution can be translated to different levels of order in films prepared by spin casting. FETs with improved performance can therefore be easily fabricated. It is also worth noting that **P1** corresponds to a class of narrow bandgap conjugated polymers under investigation for use in polymer solar cells.[27]

The synthesis of **P1** has appeared in the literature.[28] The specific sample used in our studies had a number average molecular weight of 25 kg/mol and a molecular weight distribution with a polydispersity of 1.9.[29] Solubility determinations by measuring the UV-vis absorption of saturated solutions at room temperature gave the following values: (9.5 ± 0.5) mg mL^{-1} in chlorobenzene, (8.9 ± 0.7) mg mL^{-1} in chloroform, (2.7 ± 0.2) in tetrahydrofuran (THF), and (2.3 ± 0.4) mg mL^{-1} in toluene.

The aging process involves starting from a fully solvated sample at 100 °C, followed by cooling to room temperature and allowing the solution to stand for a given period of time. Figure 1b–e show the UV-vis absorption spectra of dilute **P1** solutions (3.0×10^{-2} mg mL^{-1}) in different solvents as a function of aging time. With increasing time, one observes the emergence of a lower energy band in the 780 ~ 800 nm range. This process is more pronounced for THF and toluene, which are less effective at solvating the polymer, compared to chloroform and chlorobenzene. For example, the ratios of the intensities in the absorption band at the maximum (λ_{max}) relative to that at 725 nm after equilibration for 28 days are 1.25, 1.24 for THF and toluene, respectively, and 1.06, and 1.07 for chloroform and chlorobenzene, respectively. There is therefore a greater fraction of the chains in the aggregated state in the marginal solvents.[30] We attribute the emergence of the red-shifted peak to a transition from a well solvated situation, with poorly associated chains, to conditions where the formation of self-assembled multichain aggregates takes place.[31–33]

We now examine how the aging process in toluene leads to modifications in the bulk morphology. A higher concentration (0.5 wt%), relative to conditions in Figure 1, was required to obtain homogenous films. Atomic force microscopy (AFM) was used to image the surface morphologies obtained under identical spin casting conditions (**Figure 2**). Films prepared from precursor solution with 0–9 hour aging time were found to have approximately the same thicknesses, in the range of 25–28 nm. Films from longer aged solution have thicknesses of ~30–35 nm, as measured by ellipsometry. Figure 2 shows that aging for 3 days leads to increased density of fiber-like features on the surface. Note that the data in Figure 2 were obtained under the AFM's phase imaging mode, which visualizes

Dr. Y. D. Park, J. K. Park, Dr. J. H. Seo , Dr. J. D. Yuen, Prof. G. C. Bazan
Departments of Chemistry & Biochemistry
Department of Materials
Center for Polymers and Organic Solids
University of California
Santa Barbara, CA 93106, USA
E-mail: bazan@chem.ucsb.edu
W. H. Lee, Prof. K. Cho
Department of Chemical Engineering
Polymer Research Institute
Pohang University of Science and Technology
Pohang 790–784, Korea

DOI: 10.1002/aenm.201000005

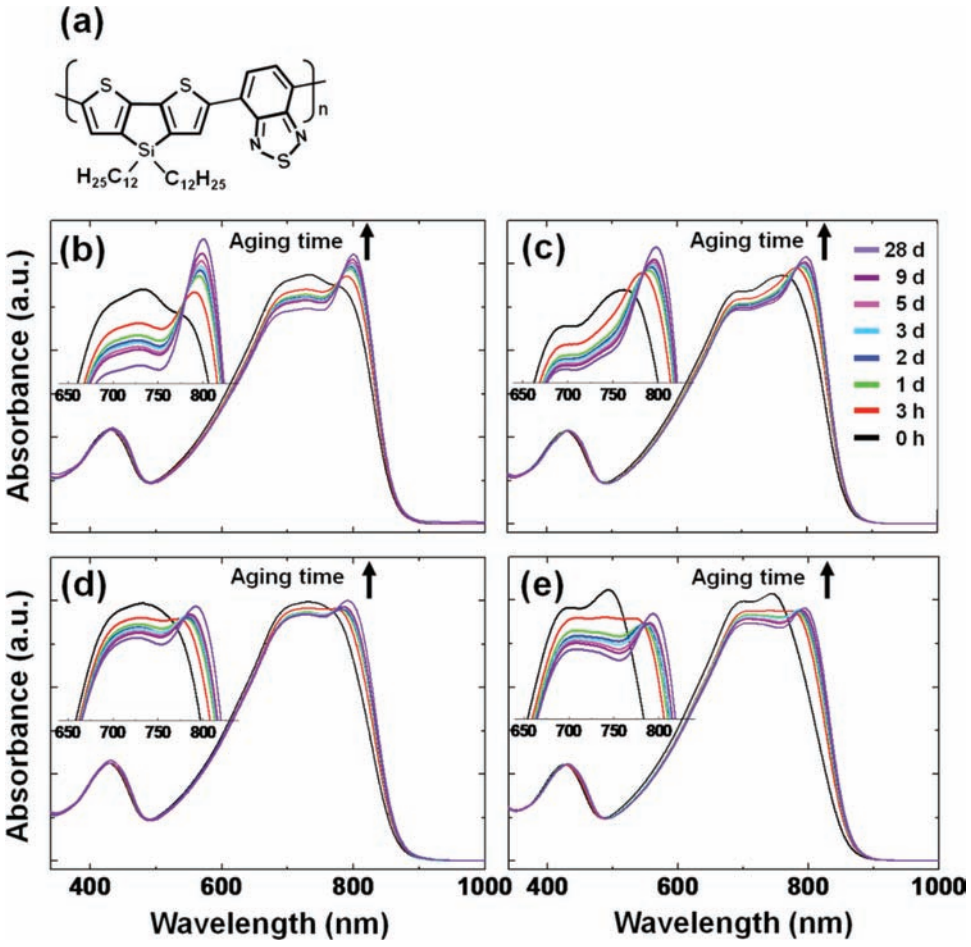

Figure 1. a) Molecular structure of **P1**. Normalized UV-vis absorption spectra of the dilute **P1** solutions (3.0×10^{-2} mg mL^{-1}) in various solvents for various aging time from 0 h to 28 days (0 h, 3 h, 1 day, 2 days, 3 days, 5 days, 9 days, and 28 days): b) THF, c) toluene, d) chloroform, and e) chlorobenzene. The insets show the magnified intensities of the maximum absorption bands. Aging time increases in the direction of the arrows.

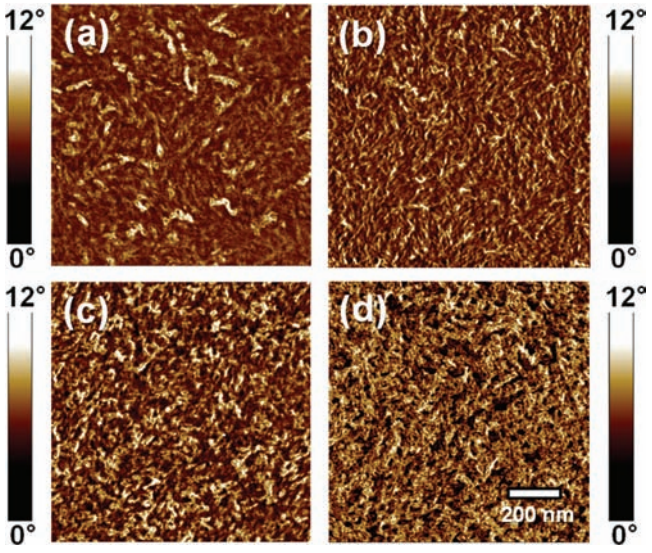

Figure 2. Tapping mode AFM phase images of **P1** films prepared from 0.5 wt% toluene solutions with various aging times: a) as-prepared, b) 1 h, c) 1 day, and d) 3 days.

hard-soft contrast in the material.[34] We attribute the contrast to differences in crystalline and amorphous regions of **P1**. Therefore, the AFM data indicate increased crystallinity of the material as a result of the controlled aggregation in solution prior to casting the film.[35]

FETs were prepared to test how modifications in the structural order of **P1** impact electronic properties by examination of the charge carrier mobilities. Devices were fabricated by using gold bottom contacts, a doped Si bottom gate, and a SiO_2 dielectric treated with hexamethyldisilazane. Typical source-drain current (I_{DS}) vs. source-drain voltage (V_{DS}) plots at five different gate voltages (V_G) as a function of aging time are shown in **Figure 3**a. A clear progression to higher currents is observed as the precursor solution is allowed to stand up to 24 h prior to film deposition. For example, the saturation current reaches a value of −14 μA at V_G = −60 V for FETs obtained from as-prepared solutions. After 1 day of aging, the saturation current at V_G = −60 V increases to −64 μA. More detail can be obtained from the transfer characteristics in Figure 3b. The average field-effect mobility of each device was calculated in the saturation regime (V_{DS} = −60 V) by plotting the square root of the drain current versus the gate voltage and fitting the data using the following equation:[36]

$$I_{DS} = \frac{WC_i}{2L}\mu(V_G - V_T)^2$$

Figure 3c summarizes the average field-effect charge carrier mobilities and on/off ratios as a function of aging time. The highest average field-effect mobility (5.0×10^{-2} $cm^2V^{-1}s^{-1}$) was observed with a **P1** film obtained after aging for 24 hours. This performance is over 5-fold greater than that of the film cast from the as-prepared solution (9.0×10^{-3} $cm^2V^{-1}s^{-1}$). This increase in field-effect mobility is attributed to improved interchain order, which will be discussed in more detail below. The current on/off ratios of the devices are on the order of $10^4 \sim 10^5$.

Allowing the 0.5 wt% toluene solutions of **P1** to age for longer than 24 hours does not improve the FET characteristics (Figure 3c). Such prolonged periods of aging lead to partial precipitation of the polymer as shown by simple visual inspection device

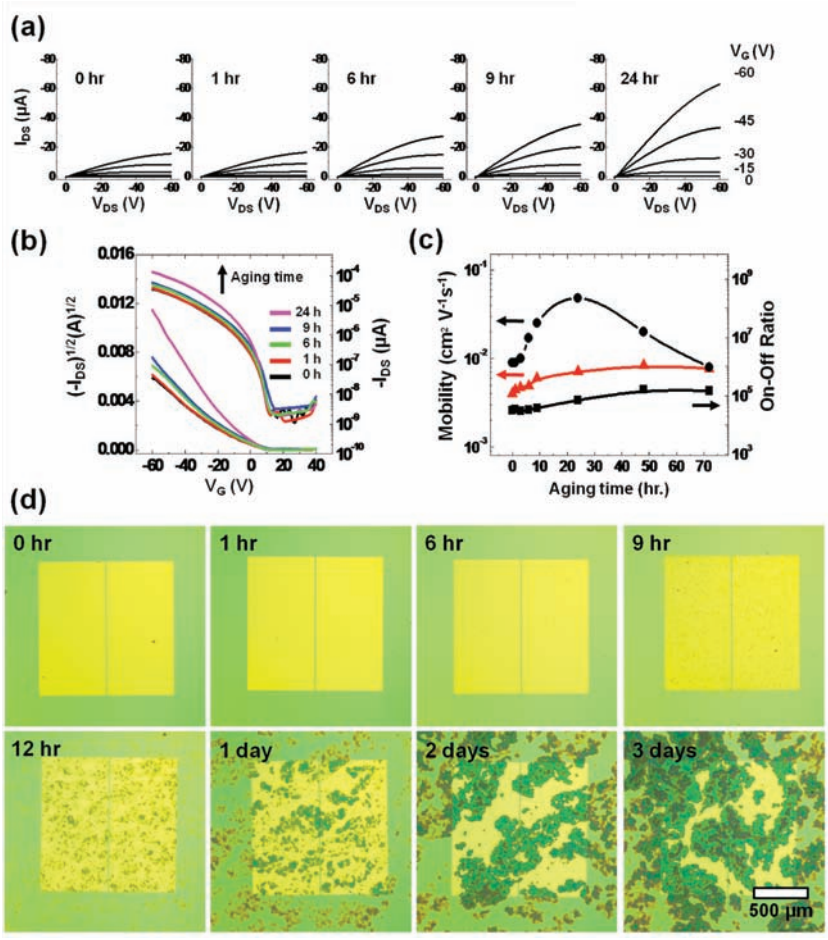

Figure 3. a) Current–voltage output characteristics of the **P1** FETs prepared from 0.5 wt% toluene solutions with various aging time. (0 h, 1 h, 6 h, 9 h, and 24 h from left.) b) Plot of $-I_{DS}$ versus V_G at a fixed V_{DS} of –60 V on both linear (left axis) and log (right axis) scales for the **P1** FETs prepared from 0.5 wt% toluene solutions. (0 h, 1 h, 6 h, 9 h, and 24 h as the aging time increases.) c) Field-effect mobility (left axis, • toluene, ▲ chlorobenzene) and on/off ratio (right axis, ■ toluene) obtained in the saturation regime of **P1** FETs as a function of the aging time. d) Optical microscopy (OM) images of the **P1** films prepared from 0.5 wt% toluene solutions with respect to aging time: as-prepared, 1 h, 6 h, 9 h, 12 h, 1 day, 2 days, and 3 days on gold electrodes/SiO_2.

photographs shown in Figure 3d. Prior to 12 h aging, the films are homogenous. From this point, there is a progressive accumulation of what appears to be polymer precipitate on the surface. Such features could be the result of precipitation prior to the spin-casting step or to aggregates in solution serving as cystallization sites during film formation. Interestingly, the best performance with solutions aged for 24 h corresponds to an intermediate situation where the formation of these precipitates is apparent on the device surface, but not as pronounced as when the solution is allowed to stand for 3 days.

Figure 3c also contains the mobilities obtained from FETs for which the **P1** layer was obtained from a good solvent, namely chlorobenzene. We note that the mobilities are lower. Moreover, there is a less pronounced effect by the aging time; a feature that we ascribe to the less pronounced tendency for the polymer chains to assemble together in a good solvent.

Insight into the inner structure within **P1** films was sought by using grazing-incidence wide angle X-ray scattering (GIWAXS). These experiments focused on the effect of aging on a 0.5 wt% toluene solution because of the relevance to the FET results in Figure 3. The grazing incidence angle was fixed at 0.18° to be above the critical angle for total reflection from the **P1** films, but below the critical angle (0.23°) of the SiO_x substrate.[21,29] We focus our attention to films obtained up to 9 hours of aging since these are homogenous. As shown in Figure 3d longer aging times lead to significant variations in film roughness, which can disrupt the internal electric filed established by the incident x-ray beam and lead to very different scattering intensities and difficulties in quantitative comparisons; data for longer aging times can be found in the Supporting Information. **Figure 4**a shows the GIWAXS pattern from a **P1** film that was obtained without aging, i.e. 0 hr. Looking at the one dimensional out of plane plots in Figure 4c, one finds that the first Bragg peak (100) at $2\theta = 4.0°$ due to the lamellar layer structure (22.1 Å)[28] is relatively weak for the as-prepared **P1** thin film. As the aging time increases, the (100) reflection becomes more pronounced with time, consistent with increased order. Additionally, that no other diffraction peaks are observed in the out-of-plane X-ray diffraction pattern except for the (l00) reflection indicates a preference for the **P1** chains to orient with alkyl groups pointing toward the substrate surface, as illustrated in Figure 4b.[17]

Weaker and less well-defined in-plane (010) peaks, corresponding to periodicities of 3.55 Å, can be observed in Figure 4a. These reflections originate from the π–π stacking of the polymer chains and are stronger for the films prepared after aging. These observations agree with a biaxial texture, having the π-stack oriented parallel and the lamellar stack oriented normal relative to the gate dielectric surface. This π–π stacking orientation is consistent with the higher mobilities observed in the FET measurements,[37,38] although the exact structural details at the dielectric/organic interface are not available at this point.

In summary, the properties of **P1** can be controlled by taking advantage of time-dependent aggregation in a solvent of intermediate quality. This self-assembly process within a fluid medium translates into thin films with higher crystallinity and internal order. Concomitant with the improved order, one finds that the charge carrier mobilities increase in FETs. Care must be taken so that the aging time is not sufficiently long so that aggregate size increases to the point of incipient precipitation, which leads to heterogeneous films with coarse features. The overall procedure yields organic semiconducting thin films with improved properties while taking advantage of a simple to use spin coating deposition method.

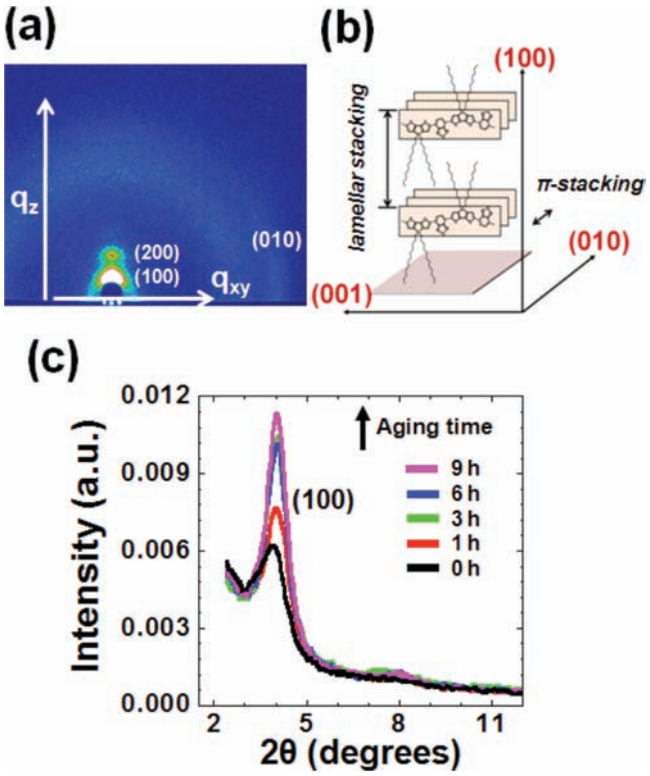

Figure 4. a) GIWAXS images representing the two-dimensional distribution of scattered X-rays for a spin-coated **P1** film on a SiO_2/Si substrate. The vertical (horizontal) axes correspond to scattering out of (in) the plane of the film prepared from the as prepared 0.5 wt% toluene solution. b) Schematic representation of the edge-on structure in **P1**. c) Out-of-plane GIWAXS of **P1** films on SiO_2/Si substrates prepared from 0.5 wt% toluene solutions depending on the aging time as a function of the scattering angle 2θ: 0 h, 1 h, 3 h, 6 h, and 9 h. The aging time increases in the direction of the arrow.

Experimental Section

Field-effect transistors with a bottom-gate, bottom-contact geometry were fabricated by using heavily doped n-type Si wafers as the gate electrodes and a 150 nm thick thermally grown silicon dioxide (SiO_2) layer (capacitance = 20 nF cm^{-2}) as the gate dielectric. The gold source and drain electrodes were structured in bottom-contact transistors with 10 µm channel length and channel width 1000 µm. A 3 nm-thick of titanium layer was used for an adhesion of the gold electrodes.

Hexamethyldisilazane (HMDS) was used as an interlayer material between the organic active material and the dielectric layer. For solution aging experiments, a 0.5 wt% toluene solution (4.4 mg mL^{-1}) was kept to 100 °C and was then cooled down to room temperature. The aged solution was spin coated at 2000 rpm onto the pre-patterned source/drain electrodes with a regular interval time to yield **P1** thin films with thicknesses of 25–35 nm. All films were fabricated inside a nitrogen atmosphere glovebox.

The solubility **P1** was determined by dissolving in each solvent of THF, toluene, chloroform and chlorobenzene. The solutions were then stirred for 4 days at room temperature, filtered and the UV-vis absorption spectra were recorded. The concentration in each solvent was calculated by using Beer's law. Solution state UV-vis absorption spectra were recorded on a Beckman Coulter DU 800 series spectrophotometer at room temperature. AFM images were obtained inside a N_2-atmosphere glove box using a multimode microscope with a Nanoscope IIIa controller (Veeco). GIWAXS experiments were carried out at the 4C2 and 8C1 beamlines (wavelength approx. 1.54 Å), at the Pohang Accelerator Laboratory (PAL), Korea. Film thicknesses were determined with an ellipsometer (M-2000V, J. A. Woollam Co., Inc.). The electrical characteristics of the FETs were measured in the accumulation mode with Keithley 4200 source/measure units at room temperature and under ambient conditions.

Acknowledgements

This work was supported by the National Research Foundation of Korea Grant funded by the Korean Government [NRF-2009–352-D00067]. We thank the NSF (DMR 0606414) and the Center for Energy Efficient Materials (CEEM) for the financial support and the Pohang Accelerator Laboratory for providing the synchrotron radiation sources at 4C2, and 8C1 beamlines used in this study.

Received: August 4, 2010
Revised: November 17, 2010
Published online: December 17, 2010

[1] J. Peet, A. J. Heeger, G. C. Bazan, *Acc. Chem. Res.* **2009**, *42*, 1700.
[2] L.-M. Chen, Z. Hong, G. Li, Y. Yang, *Adv. Mater.* **2009**, *21*, 1434.
[3] B. Kippelen, J. L. Brédas, *Energ. Environ. Sci.* **2009**, *2*, 251.
[4] B. C. Thompson, J. M. J. Fréchet, *Angew. Chem. Int. Ed.* **2008**, *47*, 58.
[5] P. K. H. Ho, J.-S. Kim, J. H. Burroughes, H. Becker, S. F. Y. Li, T. M. Brown, F. Cacialli, R. H. Friend, *Nature* **2000**, *404*, 481.
[6] M. S. Liu, Y.-H. Niu, J. Luo, B. Chen, T.-D. Kim, J. Bardecker, A. K.-Y. Jen, *Polym. Rev.* **2006**, *46*, 7.
[7] H. N. Tsao, K. Müllen, *Chem. Soc. Rev.* **2010**, *39*, 2372.
[8] Y. D. Park, J. A. Lim, H. S. Lee, K. Cho, *Mater. Today* **2007**, *10*, 46.
[9] I. McCulloch, M. Heeney, M. L. Chabinyc, D. DeLongchamp, R. J. Kline, M. Cölle, W. Duffy, D. Fischer, D. Gundlach, B. Hamadani, R. Hamilton, L. Richter, A. Salleo, M. Shkunov, D. Sparrowe, S. Tierney, W. Zhang, *Adv. Mater.* **2009**, *21*, 1091.
[10] R. J. Kline, M. D. McGehee, *Polym. Rev.* **2006**, *46*, 27.
[11] F. J. M. Hoeben, P. Jonkheijm, E. W. Meijer, A. P. H. J. Schenning, *Chem. Rev.* **2005**, *105*, 1491.
[12] G. C. Bazan, *J. Org. Chem.* **2007**, *72*, 8615.
[13] H. Sirringhaus, *Adv. Mater.* **2005**, *17*, 2411.
[14] J.-L. Brédas, J. P. Calbert, D. A. da Silva Filho, J. Cornil, *Proc. Natl. Acad. Sci. U. S. A.* **2002**, *99*, 5804.
[15] S. Berson, R. D. Bettignies, S. Bailly, S. Guillerez, *Adv. Funct. Mater.* **2007**, *17*, 1377.
[16] P.-T. Wu, H. Xin, F. S. Kim, G. Ren, S. A. Jenekhe, *Macromolecules* **2009**, *42*, 8817.
[17] K. J. Ihn, J. Moulton, P. Smith, *J. Polym. Sci, Part B: Polym. Phys.* **1993**, *31*, 735.
[18] A. J. Moulé, K. Meerholz, *Adv. Mater.* **2008**, *20*, 240.
[19] L. Li, G. Lu, X. Yang, *J. Mater. Chem.* **2008**, *18*, 1984.
[20] Z. Bao, A. Dodabalapur, A. J. Lovinger, *Appl. Phys. Lett.* **1996**, *69*, 4108.
[21] D. H. Kim, Y. D. Park, Y. Jang, H. Yang, K. Cho, Y. H. Kim, J. I. Han, D. G. Moon, S. Park, T. Chang, C. Chang, M. Joo, C. Y. Ryu, *Adv. Funct. Mater.* **2005**, *15*, 77.
[22] Y. D. Park, D. H. Kim, Y. Jang, J. H. Cho, M. Hwang, H. S. Lee, J. A. Lim, K. Cho, *Org. Electron.* **2006**, *7*, 514.
[23] J. Jo, S.-S. Kim, S.-I. Na, B.-K. Yu, D.-Y. Kim, *Adv. Funct. Mater.* **2009**, *19*, 866.
[24] G. Li, Y. Yao, H. Yang, V. Shrotriya, G. Yang, Y. Yang, *Adv. Funct. Mater.* **2007**, *17*, 1636.
[25] C. Di, K. Lu, L. Zhang, Y. Liu, Y. Guo, X. Sun, Y. Wen, G. Yu, D. Zhu, *Adv. Mater.* **2010**, *22*, 1273.

[26] J. Liu, E. E. Sheina, T. Kowalewski, R. D. McCullough, *Angew. Chem. Int. Eng.* **2002**, *41*, 329.
[27] Y.-J. Cheng, S.-H. Yang, C.-S. Hsu, *Chem. Rev.* **2009**, *109*, 5868.
[28] R. C. Coffin, J. Peet, J. Rogers, G. C. Bazan, *Nat. Chem.* **2009**, *1*, 657.
[29] M. Tong, S. Cho, J. T. Rogers, K. Schmidt, B. B. Y. Hsu, D. Moses, R. C. Coffin, E. J. Kramer, G. C. Bazan, A. J. Heeger, *Adv. Funct. Mater.* **2010**, **20**, 3959.
[30] J. Peet, N. S. Cho, S. K. Lee, G. C. Bazan, *Macromolecules* **2008**, *41*, 8655.
[31] J. K. Lee, W. L. Ma, C. J. Brabec, J. Yuen, J. S. Moon, J. Y. Kim, K. Lee, G. C. Bazan, A. J. Heeger, *J. Am. Chem. Soc.* **2008**, *130*, 3619.
[32] Y. D. Park, D. H. Kim, J. A. Lim, J. H. Cho, Y. Jang, W. H. Lee, J. H. Park, K. Cho, *J. Phys. Chem. C* **2008**, *112*, 1705.
[33] N. Kiriy, E. Jähne, H.-J. Adler, M. Schneider, A. Kiriy, G. Gorodyska, S. Minko, D. Jehnichen, P. Simon, A. A. Fokin, M. Stamm, *Nano Lett.* **2003**, *3*, 707.
[34] S. N. Magonov, V. Elings, M.-H. Whangbo, *Surf. Sci.* **1997**, *375*, L385.
[35] S. Hugger, R. Thomann, T. Heinzel, T. Thurn-Albrecht, *Colloid Polym. Sci.* **2004**, *282*, 932.
[36] G. Horowitz, *Adv. Mater.* **1998**, *10*, 365.
[37] H. N. Tsao, D. Cho, J. W. Andreasen, A. Rouhanipour, D. W. Breiby, W. Pisula, K. Müllen, *Adv. Mater.* **2009**, *21*, 209.
[38] H. Sirringhaus, P. J. Brown, R. H. Friend, M. M. Nielsen, K. Bechgaard, B. M. W. Langeveld-Voss, A. J. H. Spiering, R. A. J. Janssen, E. W. Meijer, P. Herwig, D. M. de Leeuw, *Nature* **1999**, *401*, 685.